Chemical Engineering & Processing: Process Intensification 142 (2019) 107546

Contents lists available at ScienceDirect

Chemical Engineering & Processing: Process Intensification

journal homepage: www.elsevier.com/locate/cep

Analysis of heat integration, intermediate reboiler and vapor recompression for the extractive distillation of ternary mixture with two binary azeotropes

Jinglian Gu[a], Xinqiang You[b,*], Changyuan Tao[a], Jun Li[a,*]

[a] School of Chemistry and Chemical Engineering, Chongqing University, Chongqing 401331, China
[b] Fujian Universities Engineering Research Center of Reactive Distillation Technology, College of Chemical Engineering, Fuzhou University, Fuzhou 350116, Fujian, China

ARTICLE INFO

Keyword:
Extractive distillation
Double-effect heat integration
Intermediate reboiler
Vapor recompression heat pump
Multi-objective optimization

ABSTRACT

Few works focus on the process intensification of extractive distillation (ED) for the separation of ternary mixture with two binary azeotropes due to its complexity. In this work, double-effect heat integration (DEHI), intermediate reboiler (IR) and vapor recompression (VRC) heat pump ED intensification processes for separating tetrahydrofuran-methanol-water mixture are proposed and optimized via multi-objective genetic algorithm to reduce the CO_2 emissions and the total annual cost. Furthermore, each of the ED intensification process is combined with the full use of the sensible heat in entrainer recycling stream. The results showed that all the proposed ED intensification processes are energy-saving than the conventional one. The combined DEHI process is the most economic since its TAC (3 years payback period) is reduced by 25.1% while the combined VRC is the most eco-friendly as its CO_2 emissions are saved by 30.4% compared with the conventional ED process.

1. Introduction

Although extractive distillation (ED) is by far the most widely applied separation technology for the separation of azeotropic mixtures, its major drawback is the high energy consumption [1–3]. Process intensification is an effective way to reduce the energy consumption of an ED process. Several ED intensification processes such as ED processes with double-effect heat integration (DEHI) [4], intermediate reboiler [5] and heat pump [6,7] have been explored for the separation of binary azeotropes whereas only a few studies on the ED intensification processes for the separation of ternary azeotropes due to its much more complexity in entrainer selection, process optimization and process control [8–10].

DEHI is to employ the top distillate stream in one column to heat the reboiler in another column, and the energy requirement is reduced as the heat is used twice meanwhile the capital investment is saved since the original condenser and reboiler are replaced by one heat exchanger [11,12]. For the separation of acetone-methanol azeotropic mixture, the DEHI process was proven to be superior to the conventional extractive distillation (CED) process [11]. On the contrary, Luo et al. [13]] showed that the TAC of DEHI process is higher than that of the CED process for separating isopropyl alcohol and Diisopropyl ether mixture. Therefore, a detailed evaluation of DEHI process for a specified system is needed. Another difficulty is that only two possible heat integration modes need to be considered for a two-column flowsheet, but six possible modes of heat integration processes should be investigated for a three-column process. In addition, each mode includes partial DEHI (PDEHI) and full DEHI (FDEHI) [14]]. This means that total twelve DEHI processes should be considered for a three-column ED process, which is complex.

Intermediate reboiler (IR) technology is to partake the energy demand of the high-pressure steam with intermediate- or low-pressure steam so as to save the energy cost. Luyben [[15]] employed the IR technology for the separation of propylene ($C3^{=}$) from normal heptane (nC7), and a 6.6% reduction of TAC was achieved. While Li et al. [5] introduced the IR technology for the separation of benzene-cyclohexane mixture and the TAC was reduced by 18.75%.

Recently, heat pump technology (HP) is frequently reported for reducing the energy requirement and the CO_2 emissions in spite of its high capital investment caused by compressor [16–20]. HP configurations include vapor compression (VC) [21,22], vapor recompression (VRC) [23,24] and bottom flashing (BF) [25–27]. Harwardt and Marquardt [28] compared the internal heat-integrated distillation columns (HIDiC) and the VRC processes, and pointed out that the VRC process is more cost efficient than the HIDiC process due to simpler equipment. Kazemi et al. [29] showed that the VRC process could reduce the TAC and the operating cost by 11.4% and 14.9% against the base case in sour water stripping. Compared with VC and BF, VRC performs better

* Corresponding authors.
E-mail addresses: youxinqiang@gmail.com (X. You), jli15@cqu.edu.cn (J. Li).

https://doi.org/10.1016/j.cep.2019.107546
Received 21 January 2019; Received in revised form 7 May 2019; Accepted 26 May 2019
Available online 27 May 2019

[7,16,30,31] in terms of economic but based on the electricity price [32] and the temperature difference [33]. Much high electricity price and temperature difference would lead to the rapid increase of energy cost, capital cost and TAC, which may offset the benefit of a VRC process.

For the separation of THF-methanol-water ternary mixture, dimethylsulfoxide (DMSO) has been proven as a better entrainer than ethylene glycol [34]. In this study, we go one step further and focus on the three energy-saving ED intensification processes for THF-methanol-water mixture with DMSO as entrainer. Firstly, the CED process is optimized through multi-objective genetic algorithm (MOGA) by minimizing TAC and CO_2 emissions under constraints of product purities and Pareto front is obtained as the results. Secondly, three process intensification methods are investigated. (1) In DEHI ED process, for the first time, as far as we know, simultaneous optimization of the total twelve processes is realized by employing a proposed judging rule. Furthermore, a combined DEHI process is proposed by double using the heat duty of entrainer recycling stream in addition to the top distillate stream of entrainer regeneration column. (2) In intermediate reboiler ED process, a two-level procedure is firstly proposed to conduct the optimization of the location and heat duty of the intermediate reboiler based on the temperature profile of the columns and further a combined IR process is supplied by considering the sensible heat of entrainer stream. (3) In VRC ED process, four out of nine modes of VRC configurations are considered to find the optimal VRC process. It demonstrates that the order of COPs value for VRC processes is in agreement with the order of TAC value. Then, a combined VRC process is designed in which the heat duty of entrainer recycling stream is reutilized. Finally, all the above processes are compared and the optimal process is provided.

2. Evaluation criteria and optimization tool

2.1. Total annual cost

TAC is used for the evaluation of the ED process from an economic perspective. It includes capital and operating cost and is calculated by the equation as follow:

$$TAC = \frac{\text{capital cost}}{\text{payback period}} + \text{energy cost} \tag{1}$$

The calculation of capital cost [35] and its modifications [36] are shown in Table S1 in the Supporting Information.

2.2. CO_2 emissions

CO_2 emissions are adopted for the evaluation of the ED process from an environmental perspective. CO_2 is generated according to the following stoichiometric equation.

$$C_xH_y + \left(x+\frac{y}{4}\right)O_2 \rightarrow xCO_2 + \frac{y}{2}H_2O \tag{2}$$

For the calculation of CO_2 emissions, the most commonly used model is as follow [37]:

$$[CO_2]_{emiss} = Q_{fuel}\bullet Fuel_{factor} \tag{3}$$

Where, Q_{fuel} is the amount of fuel burnt, reflecting the heating device. $Fuel_{factor}$ is the fuel factor, representing the types of the fuel. $Fuel_{factor}$ and Q_{Fuel} are defined as:

$$Fuel_{factor} = \left(\frac{\alpha}{NHV}\right)\bullet\left(\frac{C\%}{100}\right) \tag{4}$$

$$Q_{fuel} = \frac{Q_{proc}}{\lambda_{proc}}\bullet(h_{proc} - 419)\bullet\frac{T_{FTB} - T_0}{T_{FTB} - T_{stack}} \tag{5}$$

Where α (= 3.67) is the molar mass content of carbon in CO_2, NHV (kJ/kg) is the net heating value of a fuel with a carbon content of C%. Heavy fuel oil is used herein, so NHV and C% equal 39,771 kJ/kg and 86.5%, respectively [37]. λ_{proc} (kJ/kg) and h_{proc} (kJ/kg) are the latent heat and enthalpy of steam (See Table S2 in the Supporting Information) delivered to the process while T_{FTB} (1800 ^OC), T_{stack} (160 ^OC) and T_0 (25 ^OC) are the flame temperature, the stack temperature and the ambient temperature. The feed water of the boiler is assumed to be at 100 ^OC with an enthalpy of 419 kJ/kg [37]. Through steam mass balance around the boiler, the relationship between the heat duty of boiler Q_{proc} and the amount of burnt fuel Q_{fuel} is shown in Eq. (5). The CO_2 emissions for the electricity power of a compressor is taken as 51.1 kg CO_2 /GJ [20], that is 184 kg CO_2/h for 1000 kW power.

2.3. Evaluation of heat pump performance

The coefficient of performance (COP) of compressor is the key criterion for evaluating HP process [38].

Plesu et al. [39] proposed a way to preliminarily judge whether the use of a heat pump could reduce the energy requirement. The simplified equation is as following:

$$COP_s = \frac{Q}{W} = \frac{T_C}{T_R - T_C} \tag{6}$$

Where Q is the reboiler duty of column, W is the work provided, T_R and T_C are the temperature (K) of reboiler and condenser. They concluded the rule that a heat pump is recommended if COPs exceeds 10, a detail evaluation is needed if it is between 5 and 10, and heat pump is harmful rather than useful for the process if it is lower than 5.

2.4. Multi-objective genetic algorithm

Multi-objective genetic algorithm (nonsorted genetic algorithm (NSGA)-II in Matlab) is employed as the optimization tool and is directly linked with rigorous process simulations carried out in Aspen Plus [40]. In this way, optimization by MOGA and rigorous simulation by Aspen Plus could work together. The objective functions TAC and CO_2 emissions are minimized over the design and operating variables. The constraints of the three products purities are all set as 0.999 while the purity of recycling entrainer is determined by minimizing objectives. The detailed expressions for the optimization of the CED and DEHI processes are displayed as follow and the variables are somewhat different:

For the CED process:

$$\begin{aligned} &\min(TAC,CO_2) = f(N_1,N_2,N_3,N_{FE},N_{F1},N_{F2},N_{F3},R_1,R_2,R_3,D_1,D_2,D_3,F_E)\\ &\text{subjectto:}x_{D1} \geq 0.999\\ &\quad x_{D2} \geq 0.999\\ &\quad x_{D3} \geq 0.999 \end{aligned} \tag{7}$$

For the DEHI process, the three operating pressures of the columns are added as variables:

$$\begin{aligned} &\min(TAC,CO_2) = f(N_1,N_2,N_3,N_{FE},N_{F1},N_{F2},N_{F3},R_1,R_2,R_3,D_1,D_2,D_3,F_E,P_1,P_2,P_3)\\ &\text{subjectto:}x_{D1} \geq 0.999\\ &\quad x_{D2} \geq 0.999\\ &\quad x_{D3} \geq 0.999 \end{aligned} \tag{8}$$

Where N_1 [5, 80], N_2 [5, 80] and N_3 [5, 80] are the total number of trays, N_{F1} [3, 70], N_{F2} [3, 70] and N_{F3} [3, 70] are the feed locations, R_1 [0.1, 10], R_2 [0.1, 10] and R_3 [0.1, 10] are the reflux ratios, D_1 [123.0, 127.0], D_2 [180.0, 200.0] and D_3 [180.0, 200.0] are the distillate rates (kmol/h), P_1, P_2 and P_3 are the operating pressures (atm) of column C1, C2 and C3, respectively. With the aim of applying our technology in one fine chemical factory, we were recommended by the engineer from that factory to keep positive pressure in order to avoid the problems of process control, difficulty in operating and instability of production caused by reduced pressure column, so P_1, P_2 and P_3 are fixed at 1 atm for the CED process while P_1 [1.0, 10.0], P_2 [1.0, 10.0] and P_3 [1.0, 10.0] are used for the DEHI process with the aim of conducting heat integration among different columns. N_{FE} [2, 60] and F_E [50.0, 3000.0] are the entrainer feed location and flow rate (kmol/h). The flow rate of the ternary azeotropic mixture is 500 kmol/h, with content of 25.0 mol % THF, 37.5 mol% methanol and 37.5 mol% water. The composition is selected according to the liquid waste from one fine chemical factory in Chongqing city.

The vapor-liquid equilibrium of THF-methanol-water-DMSO is described by the nonrandom-two-liquid (NRTL) property model with Aspen Plus built-in binary parameters (See Table S3 in the Supporting Information). For the parameters of the genetic algorithm (GA), the number of population is specified to be 20 times of the number of variables and several ratios of crossover (from 0.8 to 0.95 with step 0.05 and mutation (from 0.02 to 0.2 with step 0.02) have been tested. The results show that 0.9 for crossover and 0.1 for mutation gives good results to find the global minimum while keeping the diversity. Therefore, 400 individuals for each generation are employed and the crossover and mutation fraction are set as 0.9 and 0.1. The stop criterion is that the TAC does not decrease anymore after 50 successive generations.

3. Conventional extractive distillation process

3.1. Flowsheet description

Fig. 1 shows the flowsheet of the CED for separating THF-methanol-water mixture with DMSO as entrainer. Fresh feed and entrainer are fed in column C1, two azeotropes are broken at one time and product THF with impurities is recovered from the top of C1. The rest components are discharged as W1 from the bottom of C1.

3.2. Results of pareto front

The obtained results of Pareto front are shown in Fig. 2 which comprises 17 designs (see Table S4 in the Supporting Information for detailed computational information). The detailed parameters of designs with lowest TAC (CED-1, marked with rhombus in red in Fig. 2) and lowest CO_2 emissions (CED-2, marked with square in red in Fig. 2) are shown in Table 1.

From Fig. 2 and Table 1,(1) the direction of optimization for minimizing TAC and CO_2 emissions is not the same. This agrees with the result in the literature [41]; (2) A small increase of CO_2 emissions is deserved. Although the CO_2 emissions in CED-1 increases compared with CED-2, the total number of trays of the three columns decreases by

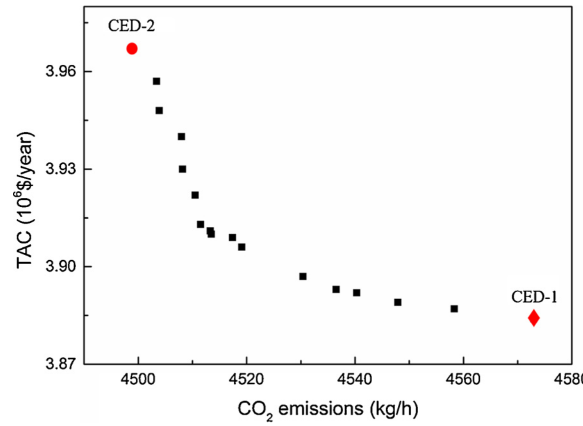

Fig. 2. TAC versus CO_2 emissions for all the designs in Pareto front of the conventional extractive distillation process.

Table 1
Optimal design of conventional extractive distillation process.

Parameter	CED-1			CED-2		
	C1	C2	C3	C1	C2	C3
N	61	34	16	71	48	18
N_{FE}	4	–	–	4	–	–
N_F	35	24	6	35	31	7
R	2.103	1.025	0.319	2.103	0.932	0.313
D (kmol/h)	125.1	187.5	187.5	125.1	187.5	187.4
F_E (kmol/h)	290.5	–	–	287.7	–	–
N_{SUM}	111			137		
Total Capital cost (10^6\$)	3.469			3.846		
Energy cost (10^6\$/year)	2.727			2.682		
CO_2 emissions (kg/h)	4573.0			4499.0		
TAC (10^6\$/year)	3.884			3.967		

Table 2
All possible DEHI configurations for three-column extractive distillation flowsheet.

Mode	1	2	3	4	5	6
PDEHI FDEHI	$Q_{C3}\rightarrow Q_{R1}$	$Q_{C3}\rightarrow Q_{R2}$	$Q_{C2}\rightarrow Q_{R1}$	$Q_{C2}\rightarrow Q_{R3}$	$Q_{C1}\rightarrow Q_{R2}$	$Q_{C1}\rightarrow Q_{R3}$

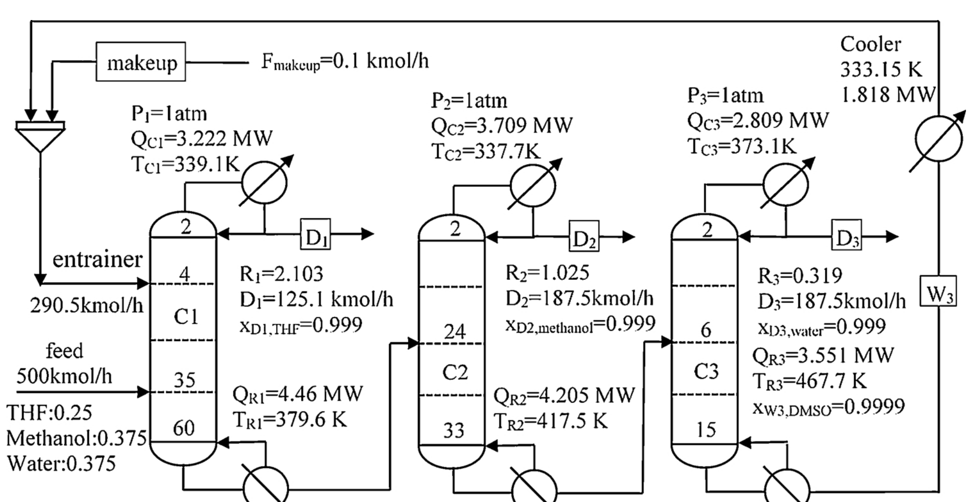

Fig. 1. Conventional extractive distillation process (CED-1) for THF-methanol-water with DMSO as entrainer.

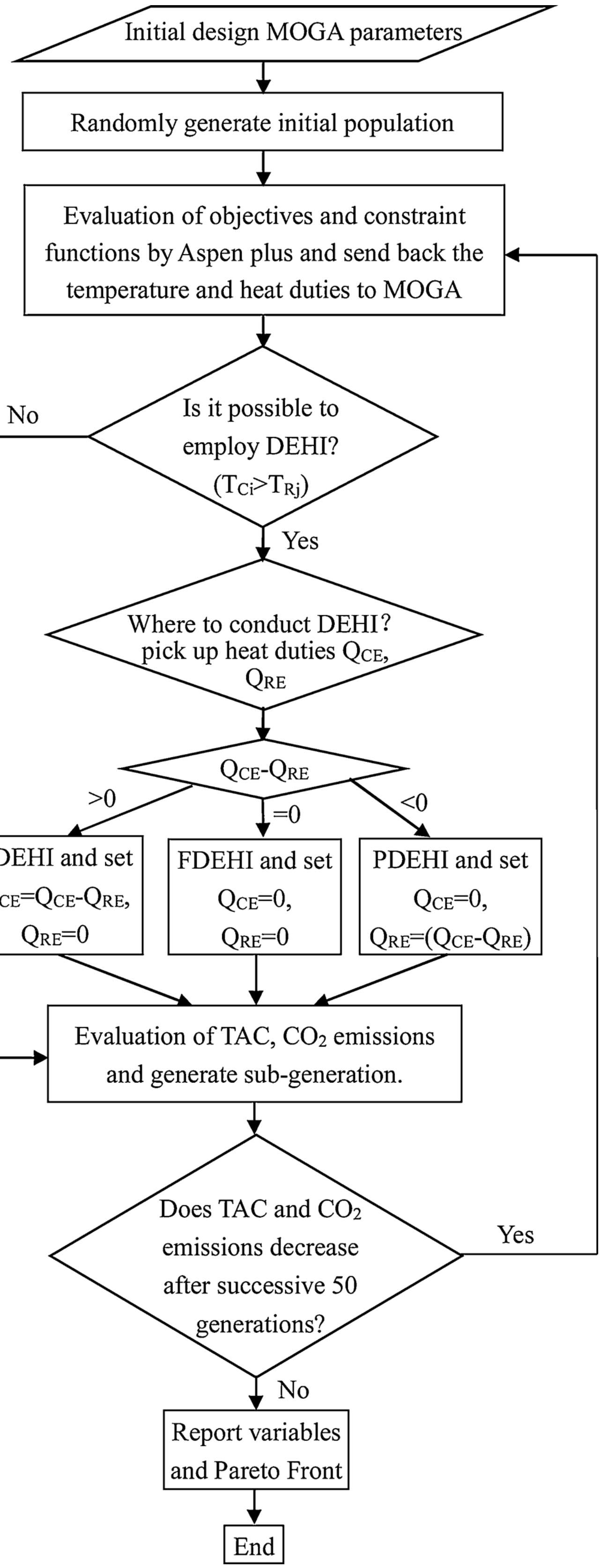

Fig. 3. Block diagram for the DEHI optimization procedure by MOGA.

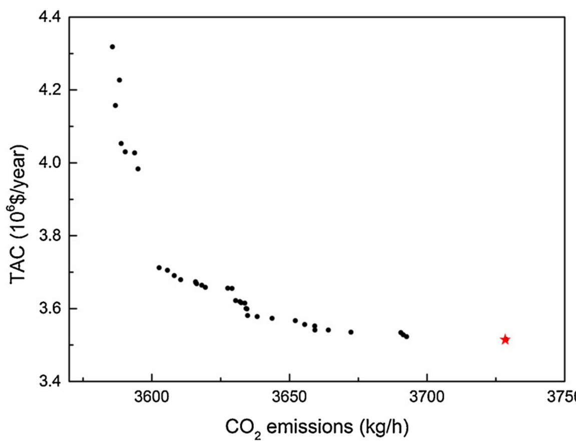

Fig. 4. Pareto front of DEHI extractive distillation designs for THF-methanol-water system.

26 and the capital cost is reduced by 9.8%, which leads to the reduction of TAC; (3) The number of trays in the rectifying section is small, which means the separation of THF from DMSO is easy and DMSO is a good entrainer for this system; (4) There are a lot of trays used in the stripping section. This is necessary for avoiding THF into the bottom stream since THF forms azeotropes with both methanol and water.

The detailed stream information as well as operational variables of CED-1 are displayed in Fig.1, which is taken as the base case for the intensified processes of IR and VRC in the following sections.

4. Process intensified extractive distillation

4.1. Extractive distillation with double-effect heat integration

4.1.1. Flowsheet description

The six DEHI configurations are named as mode 1–6 as shown in Table 2. The symbol of Q_{C3}→Q_{R1} in Table 2, for example, means that the heat is transferred from the top condenser of C3 to the bottom reboiler of C1. Further, each DEHI configuration includes partial DEHI (PDEHI) and full DEHI (FDEHI) [14]. Therefore, total 12 DEHI cases should be considered, which makes the process too complex to conduct.

In order to solve this complex issue, we try to simultaneously conduct the twelve DEHI cases by MOGA through programming. The block diagram for the DEHI optimization procedure by MOGA is shown in Fig. 3 and the programming is done as follow: first, MOGA generates randomly the seventeen variables shown in equation 10 and then sends them to Aspen plus software to conduct rigorous process simulation. After simulation, the temperatures (T_C and T_R) and heat duties (Q_C and Q_R) of the three columns and other information such as product purities and column diameters are given back to MOGA. Second, the obtained six temperatures (T_C and T_R) are ranked to judge whether it is possible to employ DEHI. If no, calculating TAC and CO_2 emissions as done for CED process and memory the results. If yes, judge where to conduct DEHI to confirm which mode it belongs to and then pick up the heat duties named Q_{CE} and Q_{RE}. Third, comparing the obtained Q_{CE} and Q_{RE} to judge whether it is full or partial DEHI. If $Q_{CE} = Q_{RE}$, it is FDEHI and both of them are set as zero when calculating TAC and CO_2 emissions. If $Q_{CE} > Q_{RE}$, it is PDEHI, Q_{CE} and Q_{RE} are set as (Q_{CE}-Q_{RE}) and zero. If $Q_{CE} < Q_{RE}$, it is also PDEHI, but Q_{CE} and Q_{RE} are set as zero and (Q_{RE}-Q_{CE}). Fourth, MOGA calculates TAC and CO_2 emissions and ranks all the populations for generating next generation until the stop criterion is satisfied. The stop criterion is that the TAC and CO_2 emissions cannot be reduced for 50 successive generations.

4.1.2. Pareto front of the DEHI process

The Pareto front is shown in Fig. 4, the red star represents the design with the lowest TAC and its detailed parameters and stream information are displayed in Fig. 5. The relationship between the operating pressure of three columns and the TAC of the designs in the Pareto front is displayed in Fig. 6.

There are 38 designs in Pareto front which satisfy the specification of product purities and the optimal design exhibits the lowest TAC. For our situation, the optimal design belongs to partial DEHI as shown in Fig. 5 and it is mode 1 from Table 2 since Q_{C3} is used to heat up Q_{R1}. Therefore, the optimal design could be named as PDEHI-1. Compared with the CED-1 process, the energy cost of the PDEHI-1 is saved by 18.3%, leading to the reduction of TAC and CO_2 emissions by 9.5% and

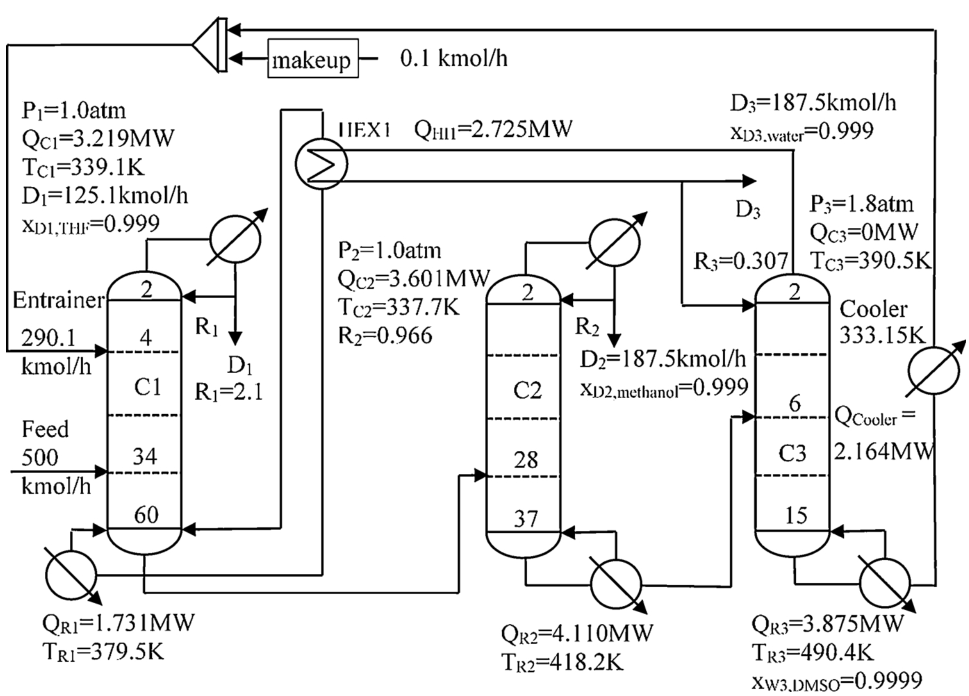

Fig. 5. Design variables and parameters of the optimal DEHI process (PDEHI-1).

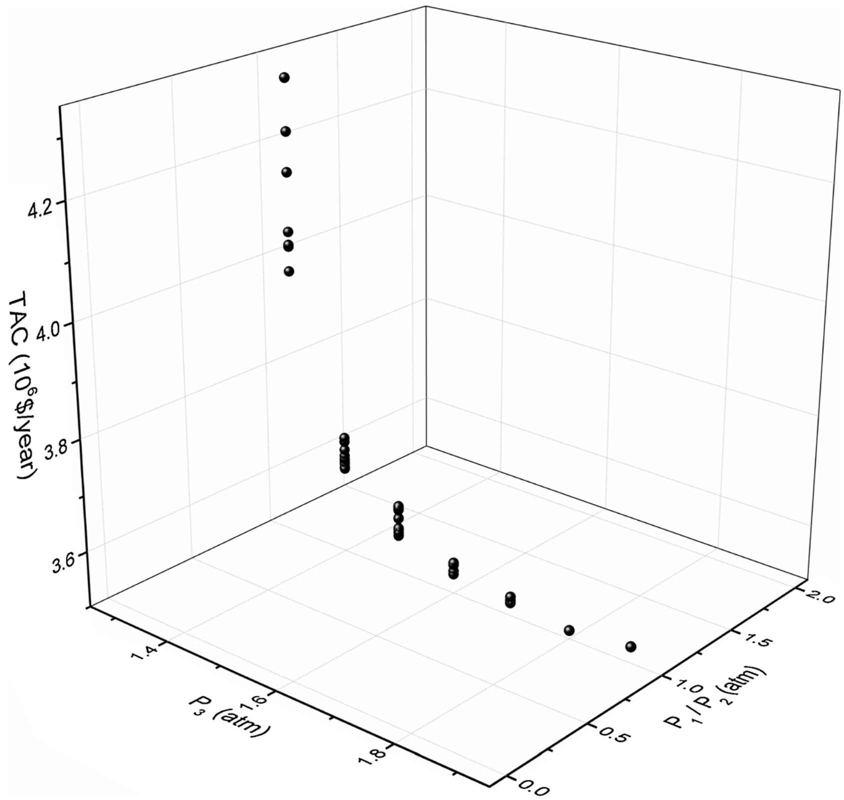

Fig. 6. Effect of P_1, P_2 and P_3 on the TAC of the DEHI processes in the Pareto front.

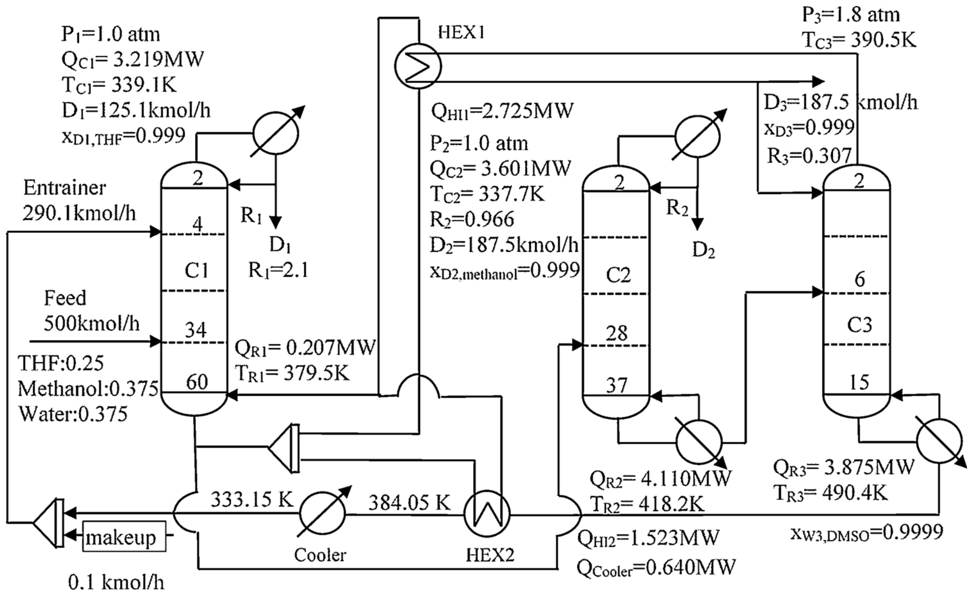

Fig. 7. Design variables and parameters of the C-DEHI process.

Table 3
Comparison of PDEHI-1 and C-DEHI ED processes.

Parameter	△T (K)	Q_{HI} (MW)	Capital cost (10^6\$)	CO_2 emissions (kg/h)	TAC (10^6\$/year)
PDEHI-1	11	2.725	3.863	3728.7	3.515
C-DEHI	11	4.248	3.894	3196.9	3.211

18.5%, respectively. The corresponding optimal integrated heat duty is 2.725 MW.

Although the initial value range of the three operating pressures are all set from atmosphere to 10 atm, only P_3 is increased while P_1 and P_2 remains at 1 atm in the Pareto front as shown in Fig. 6. This ascribes to the essence of genetic algorithm: survival of the fittest. The individuals belonging to the uneconomical cases are gradually eliminated from the genetic algorithm and the individuals belonging to the most economical case are obtained in the Pareto front.

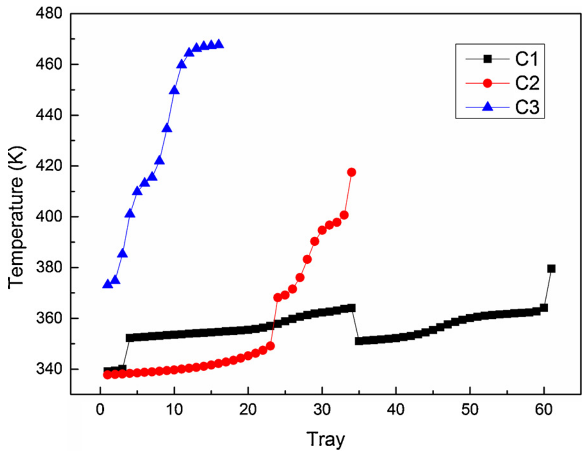

Fig. 8. Temperature profile of three columns in the CED-1 process.

4.1.3. Combined DEHI extractive distillation process

In the PDEHI-1 process, the temperature of the entrainer recycling stream which should be cooled down is 490.4 K, while the reboiler of C1 which should be heated is 379.5 K, so the temperature driving force is high enough for the heat exchange. Therefore, a combined DEHI (C-DEHI) ED process is proposed and the detailed design variables and parameters of C-DEHI are shown in Fig. 7.

The cost information of PDEHI-1 and C-DEHI are displayed in Table 3. Compared with the results of PDEHI-1 process, the proposed C-DEHI process could further reduce TAC and CO_2 emissions by 8.6% and 14.2%, respectively. This attributes to the increase (more than 1.5 times) of integrated heat duty, which leads to less energy demand in both reboiler of C1 and cooler, although the capital cost of heat exchangers increases a little.

4.2. Extractive distillation with intermediate reboiler

The temperature profiles of the three columns in CED-1 process are showed in Fig. 8 and two IR processes should be considered: IR-1 (between C1 and C3) and IR-2 (between C2 and C3).

4.2.1. Key variable and optimal results

In the IR process, the critical variables are the amount of integrated heat duty (Q_{IR}) and the location of the IR (N_{IR}), which affects each other and leads to convergence problems. Since the locations for IR technique is unavailable beforehand and there is no clear clue to infer where to conduct IR technique before obtaining the CED design, it is difficult to employ MOGA algorithm to optimize the two IR processes. To solve this issue, a two-level procedure is proposed for optimizing Q_{IR} and N_{IR} based on the optimal CED design. It works as follow: N_{IR} is regarded as decision variable and enumeration method is employed. For given N_{IR}, the discrete variables of feed locations (N_{FE}, N_{F1}, N_{F2}, N_{F3}) were listed. For specific feed locations, continuous variables (R_1, R_2, R_3, F_E) was optimized by sequential quadratic programming (SQP) method in Aspen plus by minimizing energy cost. For the minimizing energy cost design, TAC could be calculated. Level 2, each N_{IR} and its corresponding TAC could be obtained by repeat level 1. The optimal N_{IR} is found at the lowest TAC value. The result of TAC versus N_{IR} is shown in Fig. 9.

From Fig. 9, (1) The temperature driving force (△T) decreases following the increase of N_{IR}, which is in agreement with the results shown in Fig. 8. (2) At each given N_{IR}, there exists the optimal integrated heat duty Q_{IR}, and the optimal Q_{IR} value is different at different N_{IR}. This result reminds us the importance of conducting level 1 (minimizing energy cost to search for the optimal Q_{IR}). (3) The variation trends of energy cost and TAC as shown in Fig. 9c and 9d are similar because the number of trays of the two columns are limited to keep the same as the CED-1 process. (4) The highest Q_{IR} and the lowest TAC are locating at different trays for IR-1 process. Further, △T, Q_{IR}, energy cost and TAC for IR-1 and IR-2 are all different from each other. (5) IR-1 performs better than IR-2 because the TAC of the IR-1 process is lower than that of IR-2 by 5.6%. The flowsheet of the IR-1 with detail parameters is shown in Fig.10.

4.2.2. Combined IR process

In the IR-1 process, the temperature of the entrainer recycling stream is 467.7 K, which is higher than the temperature of the reboiler

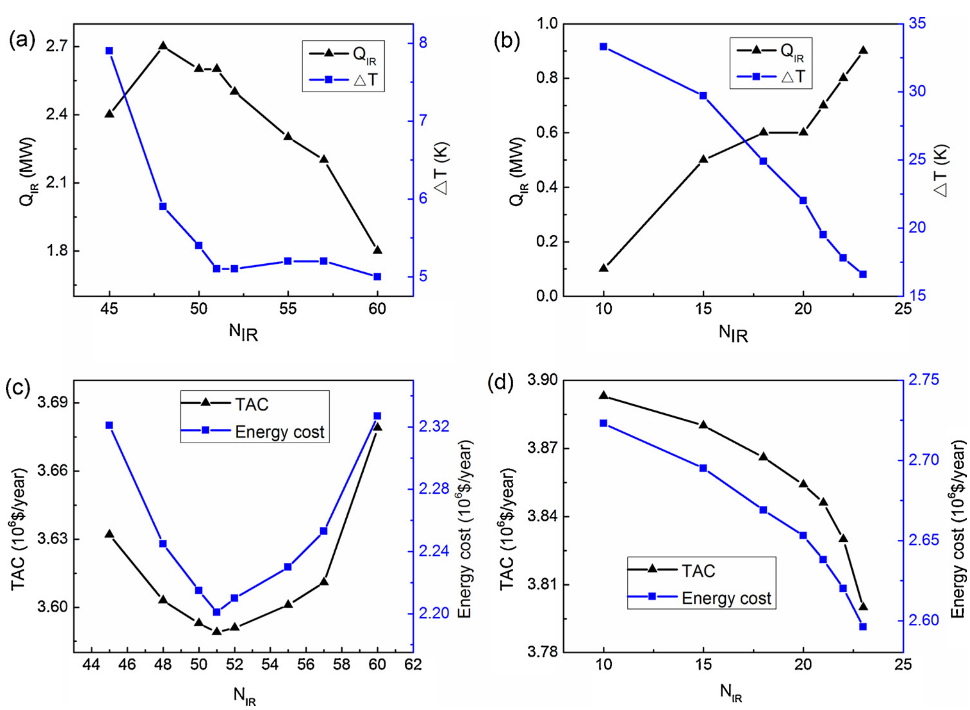

Fig. 9. Effect of N_{IR} on △T, Q_{IR}, energy cost and TAC for IR-1 (a, c) and IR-2 (b, d) processes.

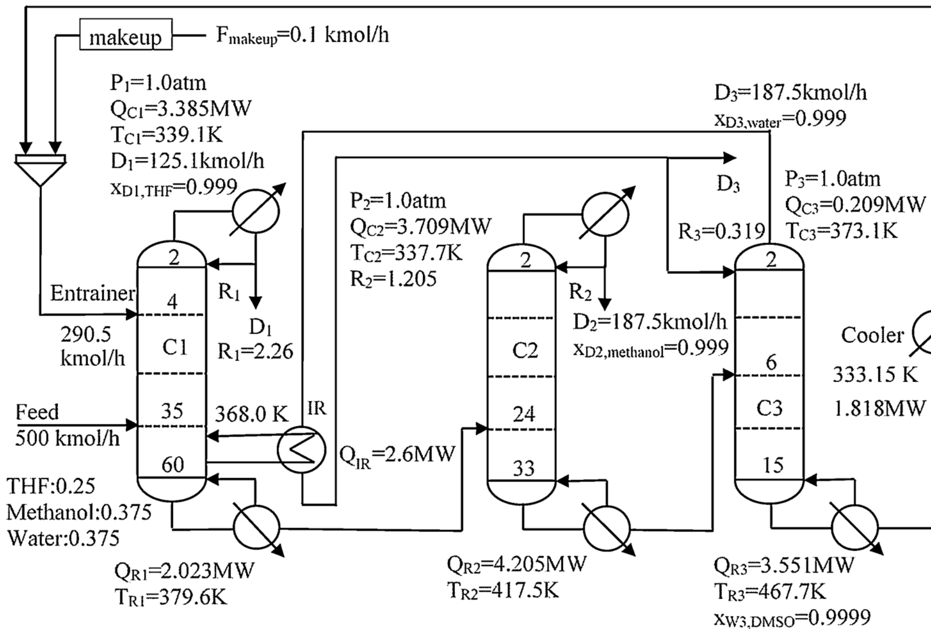

Fig. 10. Design variables and parameters of optimal extractive distillation process with intermediate reboiler (IR-1).

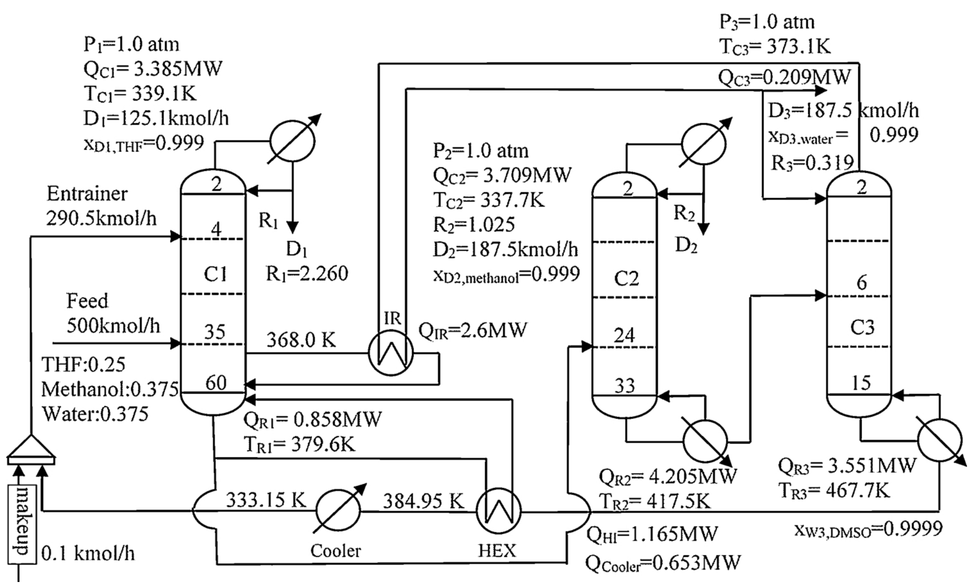

Fig. 11. Design variables and parameters of the combined IR (C-IR) process.

Table 4
Results of COPs for the CED-1 process.

Process	VRC-1	VRC-2	VRC-3	VRC-4	VRC-5	VRC-6	VRC-7	VRC-8	VRC-9
Mode	$T_{C3} \sim T_{R1}$	$T_{C2} \sim T_{R1}$	$T_{C1} \sim T_{R1}$	$T_{C3} \sim T_{R2}$	$T_{C2} \sim T_{R2}$	$T_{C1} \sim T_{R2}$	$T_{C3} \sim T_{R3}$	$T_{C2} \sim T_{R3}$	$T_{C1} \sim T_{R3}$
COPs	57.4	8.0	8.3	8.4	4.2	4.2	3.9	2.5	2.6
HP	yes	yes	yes	yes	no	no	no	no	no

in C1 (379.6 K) as shown in Fig. 10. Therefore, the entrainer recycling stream could supply heat to the reboiler in C1. A combined IR process (C-IR) is proposed on the basis of the IR-1 by using the sensible heat of the entainer recycling stream as the heat source of the reboiler of C1, and the detailed results of the C-IR are shown in Fig. 11.

Compared with the CED-1 process, the advantage of the C-IR process is that its energy cost and CO_2 emissions are reduced by 11.8% and 10.5% owing to the reutilization of the sensible heat of the entrainer recycling stream which leads to the reduction of external steam of the reboiler of C1 and the heat duty of the cooler. Although the total capital cost of the C-IR is increased by 1.2% due to the added heat exchanger (HEX as shown in Fig. 11), the TAC of the C-IR is decreased by 6.3% due to the large decrement of energy cost.

4.3. Extractive distillation with heat pump

4.3.1. Preliminary evaluation of VRC processes

Total nine modes of VRC processes as shown in Table 4 for a three-

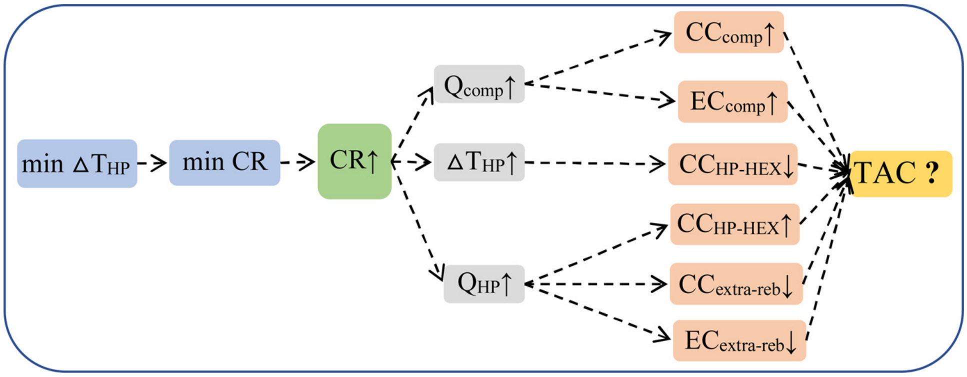

Fig. 12. Sketch of the influence of CR on TAC in a specified VRC process.

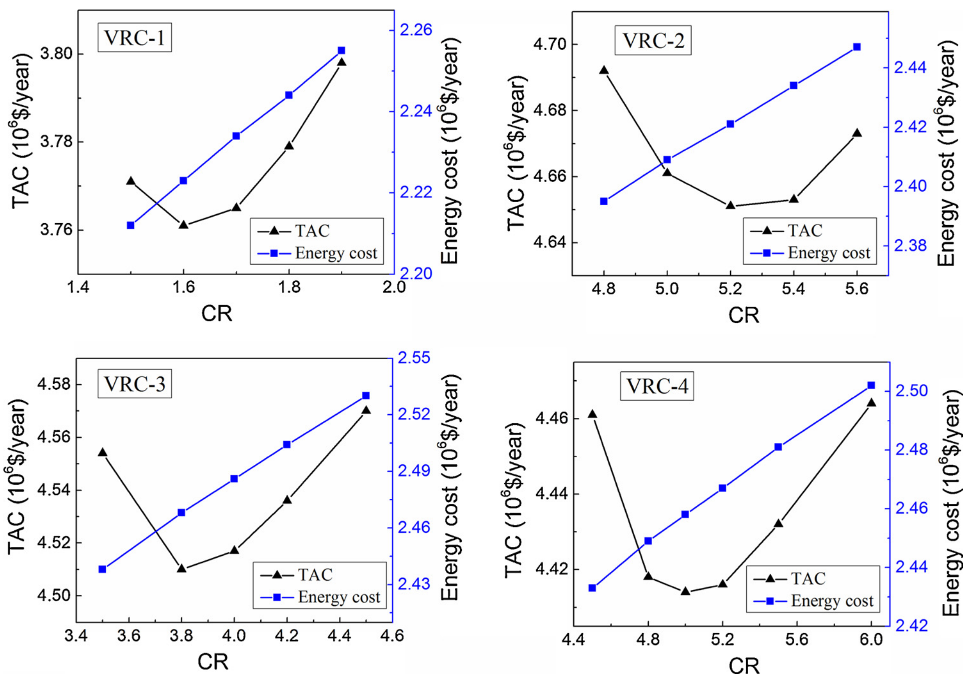

Fig. 13. TAC and energy cost versus compressor ratio of different VRC processes.

Table 5
Main parameters and cost data of different VRC processes.

Process	VRC-1	VRC-2	VRC-3	VRC-4
Q_{C1} (MW)	3.222	3.222	0	3.222
Q_{C2} (MW)	3.709	0	3.709	3.709
Q_{C3} (MW)	0	2.809	2.809	0
Q_{R1} (MW)	1.573	0.585	1.327	4.46
Q_{R2} (MW)	4.205	4.205	4.205	1.113
Q_{R3} (MW)	3.551	3.551	3.551	3.551
Q_{HP} (MW)	2.887	3.875	3.133	3.092
Q_{cooler} (MW)	1.818	1.818	1.818	1.818
Work of compressor (MW)	0.153	0.804	0.629	0.601
Qsum-CO_2 (MW)	9.482	9.145	9.712	9.725
Capital cost of compressor (10^6\$)	0.692	2.697	2.205	2.124
Energy cost of compressor (10^6\$)	0.094	0.492	0.385	0.368
Energy cost (10^6\$/year)	2.223	2.421	2.468	2.458
Capital cost (10^6\$)	4.611	6.684	6.123	5.861
CO_2 emissions (kg/h)	3593.6	3368.5	3595.3	3604.4
TAC at PP = 3 (10^6\$/year)	3.761	4.651	4.51	4.414
TAC at PP = 10 (10^6\$/year)	2.686	3.092	3.081	3.045

column flowsheet are needed to consider, which makes the optimization tedious and time-consuming. According to the simple rule proposed by Plesu et al. [39], the heat pump processes with the simplified coefficient of performance (COPs) lower than 5 are unnecessary to conduct heat pump since the temperature difference are too large to reduce the process cost. Based on the optimal design of CED-1, the COPs value between different condensers and reboilers are calculated according to Eq. 8 and the results are summarized in Table 4. It is clear that only VRC-1, VRC-2, VRC-3 and VRC-4 processes should be investigated for the studied system. One thing should be mentioned is that the MOGA could not be employed for optimizing the VRC process because the four modes in nine configurations is not clear before obtaining the optimal CED design. The four modes of VRC processes was optimized one by one based on the optimal CED design.

4.3.2. Optimization of VRC processes

For the VRC heat pump process, the compression ratio (CR, the ratio of outlet and inlet pressure of compressor) is the key parameter since it affects both the costs of compressor and heat exchanger. However, the systematic explanation about the role of CR on a VRC process has not been reported.

The sketch of the influence of CR on TAC is shown in Fig. 12. For a specified VRC process, the influence of CR on TAC is mainly reflected in the cost of the compressor and heat exchanger. In all of the feasible four VRC processes, the integrated heat duty is smaller than the heat duty of the original reboiler, which means that an extra reboiler is needed. The

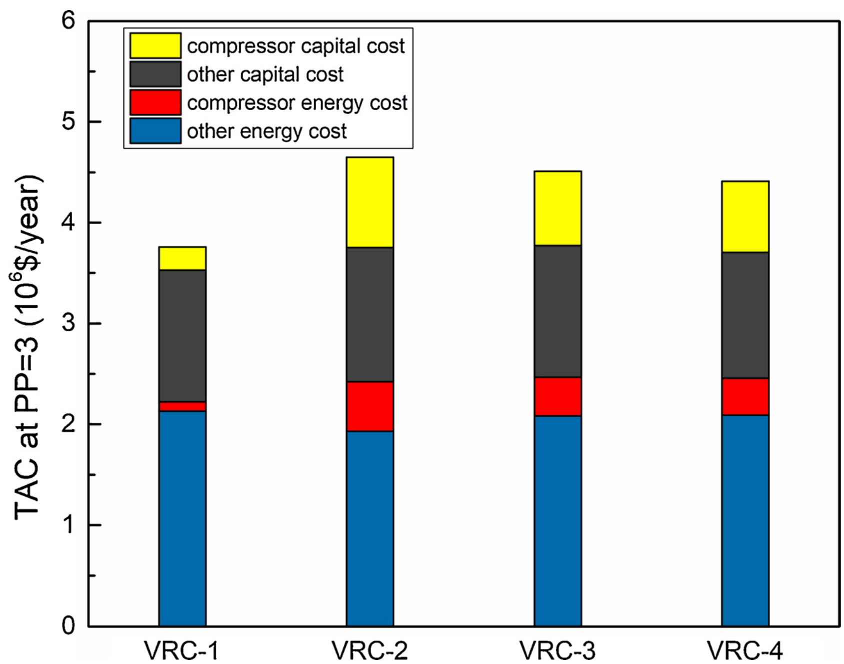

Fig. 14. Comparison of cost proportions in different VRC processes (CC: capital cost, comp: compressor).

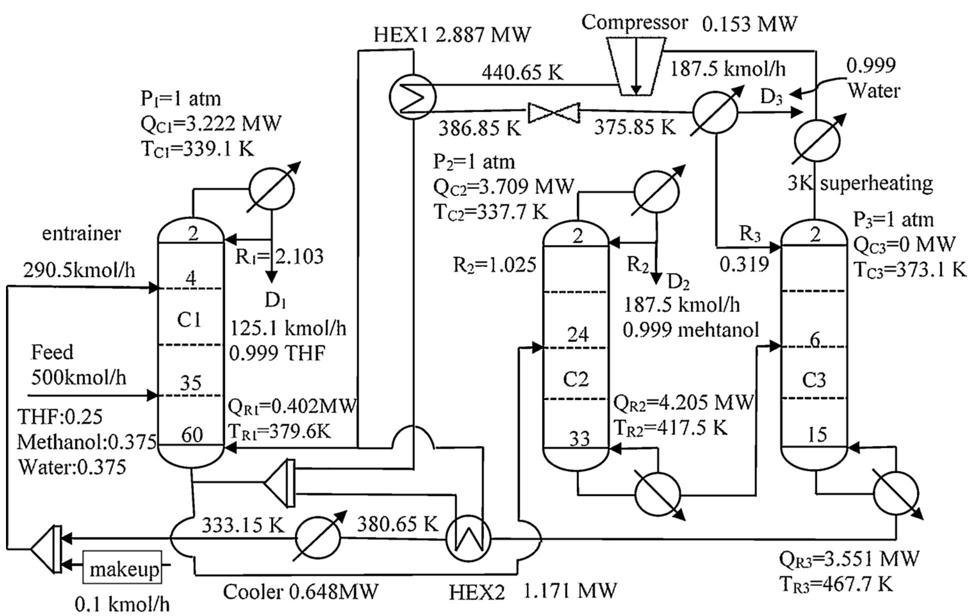

Fig. 15. Design variables and parameters of C-VRC extractive distillation process.

Table 6
Comparison of different extractive distillation processes.

Process	CED-1	C-VRC	C-IR	C-DEHI
Capital cost (10^6\$)	3.469 (0%)	4.664 (+25.6%)	4.147 (+16.3%)	3.894 (+10.9%)
Energy cost (10^6\$/year)	2.727 (0%)	1.980 (-27.3%)	1.980 (-27.3%)	1.910 (-30.0%)
TAC at PP = 3 (10^6\$/year)	3.884 (0%)	3.537(-8.9%)	3.364(-13.4%)	3.211(-17.3%)
TAC at PP = 10 (10^6\$/year)	3.075 (0%)	2.449(-20.4%)	2.397(-22.0%)	2.303(-25.1%)
CO_2 emissions (kg/h)	4573.0 (0%)	3184.9(-30.4%)	3316.0(-27.5%)	3196.9(-30.1%)

lower limit of CR is selected at that the heat integrated temperature difference ($\triangle T_{HP}$) equals about 5 K. With the increase of CR, the heat duty (Q_{comp}) of the compressor increases leading to the increase of the capital (CC_{comp}) and energy cost (EC_{comp}) of the compressor. Meanwhile, as CR increases, $\triangle T_{HP}$ increases and then leads to the decrease of the capital cost of the heat integrated exchanger ($CC_{HP\text{-}HEX}$). In addition, the value of integrated heat duty (Q_{HP}) enlarges following the increase of CR for the studied system (see Table S5 in the Supporting Information). A higher Q_{HP} would result in the increase of $CC_{HP\text{-}HEX}$ and the reduction of the capital cost ($CC_{extra\text{-}reb}$) and energy cost ($EC_{extra\text{-}reb}$)

of the extra reboiler. There should exist an optimal CR that could achieve the minimum TAC.

The optimization of CR for VRC-1, VRC-2, VRC-3 and VRC-4 processes are done by minimizing TAC (PP = 3 years) and the results are displayed in Fig. 13. From this figure, the energy cost and TAC for the four VRC processes exhibit similar trends following the increase of CR. Take VRC-1 process as example, when CR decreases, the energy cost decreases while the TAC decreases first and then increases. The decrease of energy cost is mainly due to the decrease of energy consumption of compressor1 and the extra reboiler1. The decrease of TAC is mainly contributed by the decrease of energy cost until the optimal value of CR at 1.6. If CR continues to decrease, the temperature driving force for integrated heat exchanger becomes too small, leading to the quick increase of heat transfer area and capital cost which may overcome the decrease of energy cost and exhibits the increase of TAC. The optimal CR values for VRC-2, VRC-3 and VRC-4 are 5.2, 3.8 and 5.0, respectively.

Interestingly, the order of COPs value for the four VRC processes (VRC-1 > VRC-4 > VRC-3 > VRC-2) is different from the order of optimal CR value (VRC-1 > VRC-3 > VRC-4 > VRC-2). The main reason is that the reused heat duty in VRC-3 (Q_{HP} = 3.133 MW) is bigger than that in VRC-4 (Q_{HP} = 3.092 MW). This result reminds us that more reused heat duty is helpful for conducting VRC heat pump technique while the COPs values are close.

4.3.3. Comparison of four VRC heat pump processes

The main parameters and cost data of the optimal design for VRC-1, VRC-2, VRC-3 and VRC-4 are summarized in Table 5 and Fig. 14.

From Table 5, VRC-2 is preferable from the environmental aspect due to its less CO_2 emissions resulted by the more integrated heat duty. While VRC-1 outweighs the other three from the economic view which mainly ascribes to the less energy consumption and less capital cost of the compressor (see Fig. 14) led by the small temperature difference between T_{C3} and T_{R1} (only 6.5 K). Besides, the order of COPs value for the four VRC processes (VRC-1 > VRC-4 > VRC-3 > VRC-2) is in agreement with the order of TAC value (VRC-1 < VRC-4 < VRC-3 < VRC-2), which verifies the effectiveness of COPs.

4.3.4. Combined VRC process

A new combined VRC process (C-VRC) (see Fig. 15) is designed based on the VRC-1 process. The idea is to double use the heat duty of entrainer recycling stream in addition to the heat duty of the top distillate stream of C3. Although an extra heat exchanger is added, the energy cost of the reboiler of C1 is largely decreased, the energy demand of the cooler for cooling down the entrainer recycling stream is also reduced.

Compared with VRC-1, the energy cost, CO_2 emissions and TAC (PP = 10) of the C-VRC process decreased by 10.9%, 11.3% and 8.8% although the capital cost increased by 1.1%. The results show that the C-VRC process is the best choice among all the VRC processes from the view of both economic and environmental aspects.

5. Comparison of the proposed extractive distillation processes

As shown in the above sections, the preferable choices for the double-effect heat integration, intermediate reboiler and heat pump processes are C-DEHI, C-IR and C-VRC, respectively. Thus, the results of C-DEHI, C-IR, C-VRC and CED-1 processes are summarized in Table 6 for comparison.

Compared with the CED-1 process, the proposed three process intensification techniques demonstrate great improvement in both economic and environmental aspects, which emphasizes the importance of conducting process intensification techniques for the conventional ED process. Further, all the three intensification processes give large reduction (more than 25%) in energy cost which outweighs the penalty in capital cost as shown in Table 6. Besides, this payment in capital cost becomes increasingly worthy when the payback period changes from 3-year to 10-year. For the studied system, the C-DEHI process is the best from the economic view, and it shows 25.1% reductions of TAC (PP = 10) compared with the CED-1 process. This ascribes to the 30.0% decrease of energy cost although the capital cost increases by 10.9%. From the view of environmental aspect, the three intensification processes display great reduction in CO_2 emissions and C-VRC exhibits the least CO_2 emissions.

6. Conclusion

In this work, double-effect heat integration (DEHI), intermediate reboiler (IR) and vapor recompression (VRC) heat pump techniques were systematically investigated for the separation of THF-methanol-water ternary mixture in extractive distillation and three combined processes C-DEHI, C-IR and C-VRC were proposed to further reduce the TAC (3 years payback period) and CO_2 emissions.

The results showed that all the proposed ED intensification processes demonstrate great improvement in both economic and environmental aspects compared with the optimal conventional extractive distillation process (CED-1). The combined DEHI process is the most economic which could reduce the TAC (3 years payback period) by 25.1% compared with the CED-1 process. The combined VRC process is preferable from the environmental perspective which could reduce the CO_2 emissions by 30.4%. It can be concluded that the proposed intensification process plus the full utilization of the sensible heat in the entrainer recycling stream, is an effective way to gain the economic and environmental benefits. All the proposed ED processes could be widely applied for the separation of other complex ternary azeotropic mixtures to save the valuable energy sources and pursue sustainable development.

Acknowledgments

This work was financially supported by the Fundamental Research Funds for the Central Universities (No. 2018CDYJSY0055), the National Natural Science Foundation of China (No. 21573027 to J.L., No. 21706062 to X.Q. You).

Appendix A. Supplementary data

Supplementary material related to this article can be found, in the online version, at doi:https://doi.org/10.1016/j.cep.2019.107546.

References

[1] H.K. Engelien, S. Skogestad, Selecting appropriate control variables for a heat integrated distillation system with prefractionator, Comput. Chem. Eng. 28 (2004) 683–691.
[2] A.K. Jana, Heat integrated distillation operation, Appl. Energy 87 (2010) 1477–1494.
[3] V. Tufano, Heat recovery in distillation by means of absorption heat pumps and heat transformers, Appl. Therm. Eng. 17 (1997) 171–178.
[4] L.C.B.A. Bessa, F.R.M. Batista, A.J.A. Meirelles, Double-effect integration of multicomponent alcoholic distillation columns, Energy 45 (2012) 603–612.
[5] L. Li, Y. Tu, L. Sun, Y. Hou, M. Zhu, L. Guo, Q. Li, Y. Tian, Enhanced efficient extractive distillation by combining heat–Integrated technology and intermediate heating, Ind. Eng. Chem. Res. 55 (2016) 8837–8847.
[6] A. Kazemi, A. Mehrabani-Zeinabada, M. Beheshti, Recently developed heat pump assisted distillation configurations: a comparative study, Appl. Energy 211 (2018) 1261–1281.
[7] X. You, I. Rodriguez–Donis, V. Gerbaud, Reducing process cost and CO_2 emissions for extractive distillation by double–effect heat integration and mechanical heat pump, Appl. Energy 166 (2016) 128–140.
[8] Y. Zhao, K. Ma, W. Bai, D. Du, Z. Zhu, Y. Wang, J. Gao, Energy-saving thermally coupled ternary extractive distillation process by combining with mixed entrainer for separating ternary mixture containing bioethanol, Energy 148 (2018) 296–308.
[9] C. Wang, C. Wang, Y. Cui, C. Guang, Z. Zhang, Economics and controllability of conventional and intensified extractive distillation configurations for acetonitrile/methanol/benzene mixtures, Ind. Eng. Chem. Res. 57 (2018) 10551–10563.
[10] V. Gerbaud, I. Rodriguez-Donis, L. Hegely, P. Lang, F. Denes, X. You, Review of

extractive distillation. Process design, operation, optimization and control, Chem. Eng. Res. Des. 141 (2019) 229–271.
[11] W.L. Luyben, Comparison of extractive distillation and pressure–swing distillation for acetone–Methanol separation, Ind. Eng. Chem. Res. 47 (2008) 2696–2707.
[12] J.P. Knapp, M.F. Doherty, Thermal integration of homogeneous azeotropic distillation sequences, AIChE J. 36 (1990) 969–984.
[13] H. Luo, K. Liang, W. Li, Y. Li, M. Xia, C. Xu, Comparison of pressure-swing distillation and extractive distillation methods for isopropyl alcohol/diisopropyl ether separation, Ind. Eng. Chem. Res. 53 (2014) 15167–15182.
[14] J. Gu, X. You, C. Tao, J. Li, W. Shen, J. Li, Improved design and optimization for separating tetrahydrofuran–water azeotrope through extractive distillation with and without heat integration by varying pressure, Chem. Eng. Res. Des. 133 (2018) 303–313.
[15] W.L. Luyben, Design and control of distillation columns with intermediate reboilers, Ind. Eng. Chem. Res. 43 (2004) 8244–8250.
[16] E. Díez, P. Langston, G. Ovejero, M.D. Romero, Economic feasibility of heat pumps in distillation to reduce energy use, Appl. Therm. Eng. 29 (2009) 1216–1223.
[17] N. Felbab, B. Patel, M. El-Halwagi, D. Hildebrandt, D. Glasser, Vapor recompression for efficient distillation. 1. A new synthesis perspective on standard configurations, AIChE J. 59 (2013) 2977–2992.
[18] N.V.D. Long, M. Lee, A novel NGL (natural gas liquid) recovery process based on self-heat recuperation, Energy 57 (2013) 663–670.
[19] K. Matsuda, K. Kawazuishi, Y. Kansha, C. Fushimi, M. Nagao, H. Kunikiyo, F. Masuda, A. Tsutsumi, Advanced energy saving in distillation process with self-heat recuperation technology, Energy 36 (2011) 4640–4645.
[20] M.A. Waheed, A.O. Oni, S.B. Adejuyigbe, B.A. Adewumi, D.A. Fadare, Performance enhancement of vapor recompression heat pump, Appl. Energy 114 (2014) 69–79.
[21] A. Kazemi, V. Faizi, A. Mehrabani-Zeinabad, M. Hosseini, Evaluation of performance of heat pump assisted distillation of ethanol-water mixture, Sep. Sci. Technol. 52 (2017) 1387–1396.
[22] C.J. King, Separation processes, Courier Corporation (2013).
[23] X. Gao, J. Chen, J. Tan, Y. Wang, Z. Ma, L. Yang, Application of mechanical vapor recompression heat pump to double-effect distillation for separating N, N-dimethylacetamide/water mixture, Ind. Eng. Chem. Res. 54 (2015) 3200–3204.
[24] K. Johri, G. Babu, A.K. Jana, Performance investigation of a variable speed vapor recompression reactive batch rectifier, AIChE J. 57 (2011) 3238–3242.
[25] A.K. Jana, Advances in heat pump assisted distillation column: a review, Energy Convers. Manage. 77 (2014) 287–297.
[26] A.K. Jana, Dynamic simulation, numerical control and analysis of a novel bottom flashing scheme in batch distillation, Comput. Chem. Eng. 89 (2016) 166–171.
[27] G. Karami, M. Amidpour, B.H. Sheibani, G.R. Salehi, Distillation column controllability analysis through heat pump integration, Chem. Eng. Process Process Intensif. 97 (2015) 23–37.
[28] A. Harwardt, W. Marquardt, Heat-integrated distillation columns: vapor recompression or internal heat integration? AIChE J. 58 (2012) 3740–3750.
[29] A. Kazemi, A. Mehrabani-Zeinabad, M. Beheshti, Development of a novel processing system for efficient sour water stripping, Energy 125 (2017) 449–458.
[30] Z. Fonyo, N. Benkö, Comparison of various heat pump assisted distillation configurations, Chem. Eng. Res. Des. 76 (1998) 348–360.
[31] F. Flegiel, S. Sharma, G.P. Rangaiah, Development and multiobjective optimization of improved cumene production processes, Mater. Manuf. Process 30 (2015) 444–457.
[32] J.M. Chew, C.C.S. Reddy, G.P. Rangaiah, Improving energy efficiency of dividing wall columns using heat pumps, organic Rankine cycle and Kalina cycle, Chem. Eng. Process: Process Intens. 76 (2014) 45–59.
[33] C.C.S. Reddy, Y. Fang, G.P. Rangaiah, Improving energy efficiency of distillation using heat pump assisted columns, Asia-Pac. J. Chem. Eng. 9 (2014) 905–928.
[34] J. Gu, X. You, C. Tao, J. Li, V. Gerbaud, Energy-saving reduced-pressure extractive distillation with heat integration for separating the biazeotropic ternary mixture tetrahydrofuran–Methanol–Water, Ind. Eng. Chem. Res. 57 (2018) 13498–13510.
[35] J.M. Douglas, Conceptual Design of Chemical Processes, McGraw-Hill, New York, 1988.
[36] J. Gu, X. You, C. Tao, J. Li, W. Shen, J. Li, Improved design and optimization for separating tetrahydrofuran–water azeotrope through extractive distillation with and without heat integration by varying pressure, Chem. Eng. Res. Des. 133 (2018) 303–313.
[37] M.A. Gadalla, Z. Olujic, P.J. Jansens, M. Jobson, R. Smith, Reducing CO2 emissions and energy consumption of heat-integrated distillation systems, Environ. Sci. Technol. 39 (2005) 6860–6870.
[38] O.S.L. Bruinsma, S. Spoelstra, Heat pumps in distillation, in: A.B. Haan, H. Kooijman, A. Gorak (Eds.), Proceedings Symposium Distillation and Absorption (2010) 21–28 ISBN 978-90-386-2215-6.
[39] V. Plesu, A.E. Bonet-Ruiz, J. Bonet, J. Llorens, Simple equation for suitability of heat pump use in distillation, in: J.J. Klemes, S.V. Varbanov, P.Y. Liew (Eds.), 24th European Symposium on Computer Aided Process Engineering (2014) 1327–1332 ISBN 978-0-444-63456-6.
[40] X. You, J. Gu, C. Peng, I. Rodriguez–Donis, H. Liu, Optimal design of extractive distillation for acetic acid dehydration with Nmethyl acetamide, Chem. Eng. Process. 120 (2017) 301–316.
[41] X. You, I. Rodriguez–Donis, V. Gerbaud, Investigation of separation efficiency Indicator for the optimization of the acetone − Methanol extractive distillation with water, Ind. Eng. Chem. Res. 54 (2015) 10863–10875.